Article

Infrared Spectra of Group 14 Hydrides in Solid Hydrogen: Experimental Observation of PbH, PbH, and PbH

Xuefeng Wang, and Lester Andrews

J. Am. Chem. Soc., **2003**, 125 (21), 6581-6587• DOI: 10.1021/ja029862l • Publication Date (Web): 01 May 2003

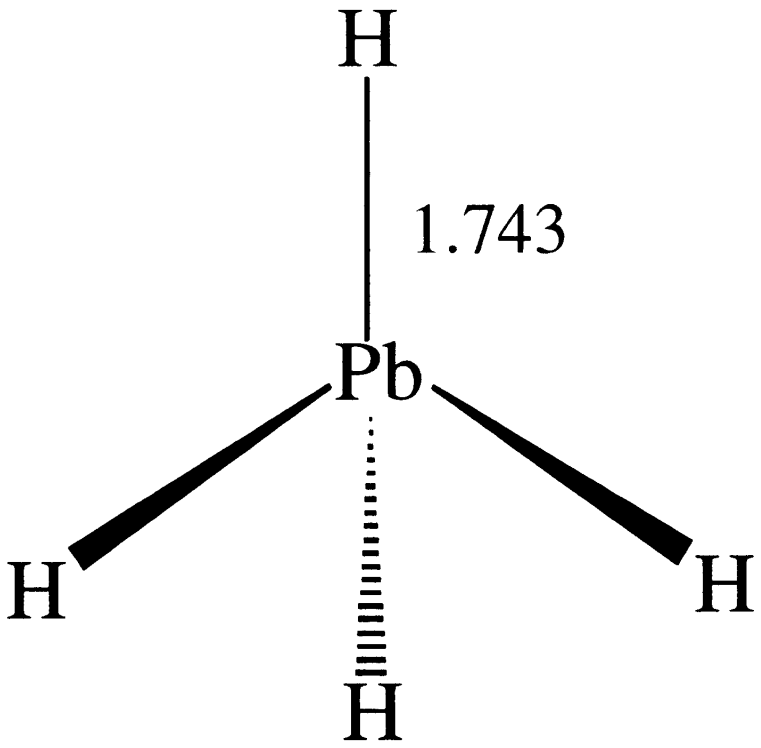

J|A|C|S
ARTICLES
Published on Web 05/01/2003

Infrared Spectra of Group 14 Hydrides in Solid Hydrogen: Experimental Observation of PbH_4, Pb_2H_2, and Pb_2H_4

Xuefeng Wang and Lester Andrews*

Contribution from the Department of Chemistry, P.O. Box 400319, University of Virginia, Charlottesville, Virginia 22904-4319

Received December 20, 2002; E-mail: lsa@virginia.edu

Abstract: Laser-ablated Si, Ge, Sn, and Pb atoms have been co-deposited with pure hydrogen at 3.5 K to form the group 14 hydrides. The initial SiH_2 product reacts completely to SiH_4, whereas substantial proportions of GeH_2, SnH_2, and PbH_2 are trapped in solid hydrogen. Further hydrogen atom reactions form the trihydride radicals and tetrahydrides of Ge, Sn, and Pb. The observation of PbH_4 at 1815 cm^{-1} and PbD_4 at 1302 cm^{-1} is in agreement with the prediction of quantum chemical calculations for these unstable tetrahydride analogues of methane. In addition, new absorptions are observed for Pb_2H_2 and Pb_2H_4, which have dibridged structures based on quantum chemical calculations.

Introduction

Lead tetrahydride, plumbane, is the most elusive and unstable member of the methane family of molecules. Although PbH_4^+ has been observed by mass spectrometry,[1] the stability of PbH_4 has been questioned.[2] Recently, the gas-phase infrared spectrum has been reported using a new synthesis of PbH_4 from $Pb(NO_3)_2$ and $NaBH_4$, with a flow reactor feed through an infrared sample cell, where plumbane decomposed to a lead film and H_2 gas in about 10 s at room temperature.[3] An antisymmetric Pb−H stretching fundamental with rotational structure was observed at 1760−1900 cm^{-1} for this short-lived tetrahedral molecule. Very recently, reactions of Pb atoms with H atoms and H_2 molecules formed PbH, PbH_2, and PbH_3 in solid neon and argon, but the reaction failed to reach PbH_4.[4] Many quantum chemical calculations, motivated by interest in relativistic effects,[5] suggest that PbH_4 is a physically stable molecule,[5−13] although the reaction of PbH_2 with H_2 is endothermic, whereas the analogous reactions for Sn, Ge, and Si are increasingly exothermic.[6−10]

Solid hydrogen has been employed as a matrix for spectroscopic investigation of trapped molecules by three groups using liquid helium at reduced pressure to cool the collecting substrate to 2 K.[14−17] The very recent condensation of Pd atoms with H_2 onto a 3 K rhodium surface[18] to form $Pd(H_2)_3$ prompted laser-ablated metal atom reactions with H_2 during condensation on a CsI optical window cooled to 3.5 K by closed-cycle refrigeration in our laboratory.[19,20] These experiments produce and trap metal hydrides, dihydrides, dihydrogen complexes, and hydrogen atoms in relatively high concentrations. We report here the infrared spectrum of PbH_4 and a comparison of the reactions of Pb, Sn, Ge, and Si atoms in condensing pure hydrogen at 3.5 K, which form hydride intermediate species that are relevant to the chemical vapor deposition process employed for semiconductor production.[21,22] In addition, we report the infrared detection of Pb_2H_2 and Pb_2H_4, which have dibridged structures[23,24] and are the lead analogues of acetylene and ethylene.

Experimental and Theoretical Methods

The laser-ablation matrix-isolation infrared spectroscopy experiment has been described previously.[25,26] Briefly, the Nd:YAG laser fundamental (1064 nm, 10 Hz repetition rate, 10 ns pulse width) was focused on rotating high purity elemental targets using 1−5 mJ/pulse, and group 14 atoms were co-deposited with pure normal H_2 or D_2 (Matheson) or a 50/50 mixture onto a CsI window cooled to 3.5 K by a Sumitomo Heavy Industries RDK-205D cryocooler. Infrared spectra were recorded in a Nicolet 750 Fourier transform instrument at 0.5 cm^{-1} resolution using liquid-nitrogen cooled MCTA and MCTB detectors after deposi-

(1) Saalfeld, F. E.; Svec, H. J. *Inorg. Chem.* **1963**, *2*, 46.
(2) Cotton, F. A.; Wilkinson, G.; Murillo, C. A.; Bochmann, M. *Advanced Inorganic Chemistry*, 6th ed.; Wiley: New York, 1999.
(3) Krivtsun, V. M.; Kuritsyn, Yu. A.; Snegirev, E. P. *Opt. Spectrosc.* **1999**, *86*, 686.
(4) Wang, X.; Andrews, L.; Chertihin, G. V.; Souter, P. F. *J. Phys. Chem. A* **2002**, *106*, 6302 (Sn, Pb + H_2).
(5) Desclaux, J. P.; Pyykkö, P. *Chem Phys. Lett.* **1974**, *29*, 534. Pyykkö, P. *Chem. Rev.* **1988**, *88*, 563.
(6) Schwerdtfeger, P.; Silberbach, H.; Miehlich, B. *J. Chem. Phys.* **1989**, *90*, 762.
(7) Dyall, K. G.; Taylor, P. R.; Faegri, K.; Partridge, H. *J. Chem. Phys.* **1991**, *95*, 2583.
(8) Dyall, K. G. *J. Chem. Phys.* **1992**, *96*, 1210.
(9) Schwerdtfeger, P.; Heath, G. A.; Dolg, M.; Bennett, M. A. *J. Am. Chem. Soc.* **1992**, *114*, 7518.
(10) Kaupp, M.; Schleyer, P. v. R. *J. Am. Chem. Soc.* **1993**, *115*, 1061.
(11) Visser, O.; Visscher, L.; Aerts, P. J. C.; Nieuwpoort, W. C. *Theor. Chim. Acta* **1992**, *81*, 405.
(12) (a) Steinbrenner, A.; Bergner, A.; Dolg, M.; Stoll, H. *Mol. Phys.* **1994**, *82*, 3. (b) Wang, S. G.; Schwarz, W. H. E. *J. Mol. Struct. (THEOCHEM)* **1995**, *338*, 347.
(13) Han, Y.-K.; Bae, C.; Lee, Y. S. *J. Chem. Phys.* **1999**, *19*, 9353.
(14) Van Zee, R. J.; Li, S.; Weltner, W., Jr. *J. Chem. Phys.* **1995**, *102*, 4367.
(15) Tam, S.; Macler, M.; Fajardo, M. E. *J. Chem. Phys.* **1997**, *106*, 8955.
(16) Momose, T.; Shida, T. *Bull. Chem. Soc. Jpn.* **1998**, *71*, 1.
(17) Li, L.; Graham, J. T.; Weltner, W., Jr. *J. Phys. Chem. A* **2001**, *105*, 11018.
(18) Manceron, L., to be published.
(19) Wang, X.; Andrews, L. *J. Phys. Chem. A* **2003**, *107*, 570 (Cr + H_2).
(20) Wang, X.; Andrews, L. *J. Phys. Chem. A* **2003**, in press (Mn + H_2).
(21) Jasinski, J. M.; Gates, S. M. *Acc. Chem. Res.* **1991**, *24*, 9.
(22) Lu, G.; Crowell, J. E. *J. Chem. Phys.* **1993**, *98*, 3415.
(23) Chen, Y.; Hartmann, M.; Diedenhofen, M.; Frenking, G. *Angew. Chem., Int. Ed.* **2001**, *40*, 2052.
(24) Trinquier, G. *J. Am. Chem. Soc.* **1990**, *112*, 2130; **1991**, *113*, 144.
(25) Hassanzadeh, P.; Andrews, L. *J. Phys. Chem. A* **1992**, *96*, 9177.
(26) Chertihin, G. V.; Andrews, L. *J. Chem. Phys.* **1996**, *105*, 2561 (Pb + O_2).

Table 1. Infrared Absorptions (cm^{-1}) Observed for Reactions of Laser-Ablated Group 14 Elements Co-deposited with Pure Hydrogen or Deuterium at 3.5 K

Si		Ge		Sn		Pb		
H_2	D_2	H_2	D_2	H_2	D_2	H_2	D_2	identification
						1501.3	1076.2	MH, site
						1497.8	1069.2	MH, site
		1834.0	1316.1	1645.5	1183.1	1494.1	1066.8	MH
		1825.3	1313.6	1643.9	1180.5	1488.3	1063.9	MH
		1858.5	1338.4			1543.7	1108.6	MH_2
		1856.4	1335.7	1669.6	1200.7	1540.7	1105.1	MH_2
		1854.5	1332.7	1665.4	1197.6	1537.1	1103.0	MH_2
		902.8	646.5			703[a]		MH_2
925.3	668.7	2093.3	1500.9	1851.7	1330.7	1692.9	1217.4	MH_3
722.9	545.7	853.5				632.3	457.2	MH_3
2183.5	1593.2	2104.9	1516.8	1899.5	1664.4	1815.0	1302.0	MH_4
908.4	670.9	816.8	590.9	677.5	486.6			MH_4
				1114.2		978.2	737.5	M_2H_2
1096.4		970.3		911.7	665.3	789.4	575.9	M_2H_2
		2035[b]	1481			1459.2[c]	1045.8[c]	M_2H_4
		2009[b]	1468			959.5[c]	702.6[c]	M_2H_4
2170.0	1580.6	2078.7						M_2H_6
2156.5	1546.0							M_2H_6
900.8	679.0							M_2H_6
837.7	619.6	750.3	542.0					M_2H_6
1841.7		1709.6				1383	995	MH_3^-
						1255.7	924.7	Pb_xH_y

[a] New weak bands in solid argon at 702 and 501 cm^{-1} track with PbH_2 and PbD_2 bands on annealing and photolysis. [b] Probably GeH_2GeH_2 isomer. [c] $HPb(\mu\text{-}H)_2PbH$ isomer, matrix splittings at 966.9 and 712.0 cm^{-1}.

tion, annealing, and filtered UV−vis irradiation. We annealed solid hydrogen samples to 6.0−6.8 K using resistance heat on the refrigerator cold stage: the samples were above 6 K for less than 30 s.

Density functional theory frequency calculations were helpful in assigning lead and platinum hydride spectra,[4,27] so similar B3LYP/6-311++G**/SDD calculations were performed for dilead hydrides.[28−31] Comparable results were obtained using the BPW91 functional.[32] Although these calculations are only approximate, they provide a useful guide for assigning vibrational spectra.

Results and Discussion

Infrared spectra from Si, Ge, Sn, and Pb atom co-condensation reactions with pure hydrogen will be reported. Table 1 compares the product absorptions, which are assigned by comparison with previous neon, deuterium, and argon matrix work.[4,33,34]

Silicon. Matrix isolation investigations were done with silicon and pure hydrogen using two laser energies, and the Si−H stretching region is illustrated in Figure 1. Not shown are the broad 4781, 4548, and 4222 cm^{-1} and sharp 4736, 4502, and 4147 cm^{-1} absorptions characteristic of solid hydrogen.[15] Very strong 2183.5 and 908.4 cm^{-1} absorptions are due to SiH_4: these bands and the 2189.4 cm^{-1} satellite, which increases on annealing, are in very good agreement with hydrogen matrix spectra of authentic SiH_4 co-deposited with hydrogen at 2 and 4 K.[17] Weak 925.3 and 722.9 cm^{-1} absorptions are due to the SiH_3 radical, and again the ν_3 fundamental of SiH_3 is covered by the strong SiH_4 absorption, but absorptions of Si_2H_6 (Table 1) are shown in the figure.[33] Additional sharp bands due to Si_2H_2 at 1096.4 cm^{-1} disappear on annealing, and those due to SiH_3^- at 1841.7 cm^{-1} disappear on photolysis (Figure 1b,c): neon matrix counterparts at 1100 and 1837 cm^{-1} behave similarly.[33] A weaker 1858.7 cm^{-1} band may also be due to SiH_3^-. The yield of Si_2H_2 in these experiments is much smaller than that produced from thermal evaporation of Si atoms in a recent investigation.[35] Note the complete absence of SiH_2 and SiH absorptions, which would appear in the 2000−1950 cm^{-1} region between the neon and argon matrix counterparts observed previously. The failure to trap SiH and SiH_2 in solid hydrogen attests to their great reactivity with H_2.

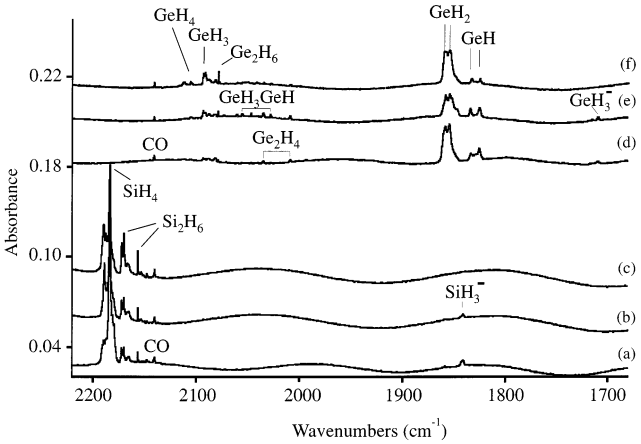

Figure 1. Infrared spectra in the 2220−1680 cm^{-1} region for laser-ablated Si or Ge co-deposited at 3.5 K for 25 min with 2.5 mmol of normal hydrogen: (a) Si + H_2, (b) after annealing to 6.3 K, (c) after $\lambda > 240$ nm irradiation, (d) Ge + H_2, (e) after annealing to 6.3 K, and (f) after $\lambda > 240$ nm irradiation.

A recent investigation of Si atom reactions with SiH_4 in excess argon reported spectra of the SiH_2SiH_2 and SiH_3SiH isomers.[36] This work shows that the 2150, 2145, 857 cm^{-1} bands previously assigned to Si_2H_4 must be due to another transient species, and SiH_3SiH is a good possibility assuming that the strong 1963 cm^{-1} band is masked by the strong SiH absorption we observed in solid argon.[33] Any SiH_2SiH_2 absorptions in pure H_2 are masked by strong SiH_4 absorptions, and the strongest SiH_3SiH absorption at 1963 cm^{-1} is clearly not observed in the present pure hydrogen experiments (Figure 1).

Germanium. Infrared spectra of germanium reaction products are shown in Figure 1d. The most obvious difference with silicon is the observation of strong GeH_2 (1858.5, 1854.5 cm^{-1}) and GeH (1834.0, 1825.3 cm^{-1}) absorptions and weak GeH_4 (2112.2, 2104.9, 816.8 cm^{-1}) and GeH_3 (2093.3, 853.5 cm^{-1}) absorptions. This demonstrates that GeH and GeH_2 are much

(27) Andrews, L.; Wang, X.; Manceron, L. *J. Chem. Phys.* **2001**, *114*, 1559 (Pt + H_2).
(28) Frisch, M. J.; Trucks, G. W.; Schlegel, H. B.; Scuseria, G. E.; Robb, M. A.; Cheeseman, J. R.; Zakrzewski, V. G.; Montgomery, J. A., Jr.; Stratmann, R. E.; Burant, J. C.; Dapprich, S.; Millam, J. M.; Daniels, A. D.; Kudin, K. N.; Strain, M. C.; Farkas, O.; Tomasi, J.; Barone, V.; Cossi, M.; Cammi, R.; Mennucci, B.; Pomelli, C.; Adamo, C.; Clifford, S.; Ochterski, J.; Petersson, G. A.; Ayala, P. Y.; Cui, Q.; Morokuma, K.; Malick, D. K.; Rabuck, A. D.; Raghavachari, K.; Foresman, J. B.; Cioslowski, J.; Ortiz, J. V.; Baboul, A. G.; Stefanov, B. B.; Liu, G.; Liashenko, A.; Piskorz, P.; Komaromi, I.; Gomperts, R.; Martin, R. L.; Fox, D. J.; Keith, T.; Al-Laham, M. A.; Peng, C. Y.; Nanayakkara, A.; Gonzalez, C.; Challacombe, M.; Gill, P. M. W.; Johnson, B.; Chen, W.; Wong, M. W.; Andres, J. L.; Gonzalez, C.; Head-Gordon, M.; Replogle, E. S.; Pople, J. A. *Gaussian 98*, revision A.7; Gaussian, Inc.: Pittsburgh, PA, 1998.
(29) (a) Becke, A. D. *J. Chem. Phys.* **1993**, *98*, 5648. (b) Stevens, P. J.; Devlin, F. J.; Chablowski, C. F.; Frisch, M. J. *J. Phys. Chem.* **1994**, *98*, 11623.
(30) (a) Krishnan, R.; Binkley, J. S.; Seeger, R.; Pople, J. A. *J. Chem. Phys.* **1980**, *72*, 650. (b) Frisch, M. J.; Pople, J. A.; Binkley, J. S. *J. Chem. Phys.* **1984**, *80*, 3265.
(31) Andrae, D.; Haussermann, U.; Dolg, M.; Stoll, H.; Preuss, H. *Theor. Chim. Acta* **1990**, *77*, 123.
(32) (a) Becke, A. D. *Phys. Rev. A* **1988**, *38*, 3098. (b) Perdew, J. P. *Phys. Rev. B* **1983**, *33*, 8822. (c) Perdew, J. P.; Wang, Y. *Phys. Rev. B* **1992**, *45*, 13244.
(33) Andrews, L.; Wang, X. *J. Phys. Chem. A* **2002**, *106*, 7697 (Si + H_2).
(34) Wang, X.; Andrews, L.; Kushto, G. P. *J. Phys. Chem. A* **2002**, *106*, 5809 (Ge + H_2).
(35) Maier, G.; Reisenauer, H. P.; Meudt, A.; Egenolf, H. *Chem. Ber.* **1997**, *130*, 1043.
(36) Maier, G.; Reisenauer, H. P.; Glatthaar, J. *Chem.-Eur. J.* **2002**, *8*, 4383.

less reactive with H_2 than their silicon analogues. Annealing to 6.3 K increased GeH_3, GeH_4, and Ge_2H_6 (2078.7, 750.3 cm^{-1}) absorptions, decreased the GeH_2 and weak 970.3 cm^{-1} bands, and increased the 2060.4, 2027.9, 771.3 cm^{-1} absorption group. Irradiation ($\lambda > 380$, $\lambda > 290$, $\lambda > 240$ nm) decreased and destroyed the GeH_3^- band (1709.6 cm^{-1}) and weak absorptions at 2009, 2028, 2035, 2047, 2055, and 2060 cm^{-1} and increased GeH_4, GeH_3, GeH_2, and Ge_2H_6 bands.[34] It appears that the most effective synthesis of GeH_4 in these experiments is through the photochemical reaction of GeH_2 and H_2. Our hydrogen matrix experiments clearly show that GeH_2 is much less reactive than SiH_2 with H_2, in agreement with flash-photolysis work.[37] Recent kinetic studies found the rate constant for the $GeH_2 + D_2$ reaction to be less than 1/260 of that for the $SiH_2 + D_2$ reaction.[38]

The 970.3 cm^{-1} absorption is just below the 972.2 cm^{-1} band assigned to dibridged Ge_2H_2 in solid neon, and this assignment is appropriate.[34] Although GeO might appear in this region, GeO in solid hydrogen should absorb above the 971.1 cm^{-1} argon matrix counterpart;[39] hence, the 970.3 cm^{-1} absorption is not due to GeO. The 2035 and 2009 cm^{-1} absorptions observed on deposition increase on annealing and decrease on photolysis, and they are probably due to GeH_2GeH_2 as assigned earlier.[34] We calculated frequencies for the GeH_3GeH isomer,[40] found to be only 0.9 kcal/mol higher than GeH_2GeH_2,[41] and obtained Ge−H stretching modes 10−15 cm^{-1} higher than those for GeH_2GeH_2 plus a strong 1864 cm^{-1} band that would be obscured by GeH_2 absorption. It is likely that the 2060 and 2028 cm^{-1} absorptions are due to the GeH_3GeH isomer formed here from the combination of GeH_3 and GeH on annealing. These bands increase on annealing, decrease on photolysis, restore on further annealing, and are destroyed by final UV photolysis.

A 50/50 H_2/D_2 experiment was done with Ge, and the strong products were observed for both isotopes as shown in Figure 2. After sample deposition, the relative intensities of GeH_2, GeH and GeD_2, GeD absorptions were approximately 2/1 for equal populations of hydrogen and deuterium products with 2/1 absolute infrared intensities (calculated). However, $\lambda > 240$ nm photolysis increased GeH_2 much more than GeD_2 (60% as compared to 20%), and final annealing favored the hydrides over the deuterides. The sharp 2081.4 and 1501.8 cm^{-1} bands are assigned to GeH_2D and $GeHD_2$, respectively, and the 2104.4 and 1518.5 cm^{-1} bands labeled 4 are due to mixed isotopic tetrahydrides.

Tin. The major tin hydride reaction products are shown in Figure 3. The sharp, strong 1645.5 cm^{-1} absorption for SnH is dominant, followed by 1669.6, 1665.4 cm^{-1} absorption for SnH_2, and a sharp 1851.7 cm^{-1} band for the SnH_3 radical. These absorptions are near the neon matrix and slightly higher than the argon matrix counterparts assigned to $SnH_{1,2,3}$, and they exhibit 1.3908, 1.3905, and 1.3914 isotopic ratios with frequencies assigned to $SnD_{1,2,3}$ in solid deuterium. Annealing to 6.3 K produces a new weak 1899.5 cm^{-1} band, increases SnH_3 absorbance a factor of 2.5, sharpens the SnH_2 band, and doubles the SnH absorbance (Figure 3b). In addition, a weak 911.7 cm^{-1} band increases 3-fold, and a new weak band appears at 677.5 cm^{-1}. A $\lambda > 470$, $\lambda > 380$, $\lambda > 290$ nm photolysis sequence slightly increases the 1899.5, 677.5 cm^{-1} bands and the 1851.7 absorption, markedly decreases the SnH_2 band, and slightly decreases the SnH and 911.7 cm^{-1} absorptions. A subsequent 6.5 K annealing slightly decreases the 1899.5, 1851.7, and 1645.5 cm^{-1} absorptions and increases the 911.7 cm^{-1} absorption. A final $\lambda > 240$ nm irradiation increases the 1899.5 cm^{-1} and SnH_2 bands and decreases the SnH and 911.7 cm^{-1} absorptions (Figure 3e).

The 1899.5 and 677.5 cm^{-1} bands are assigned to the ν_3 and ν_4 modes of SnH_4 in solid hydrogen on the basis of near agreement with the gas-phase values (1901, 677 cm^{-1})[42,43] and

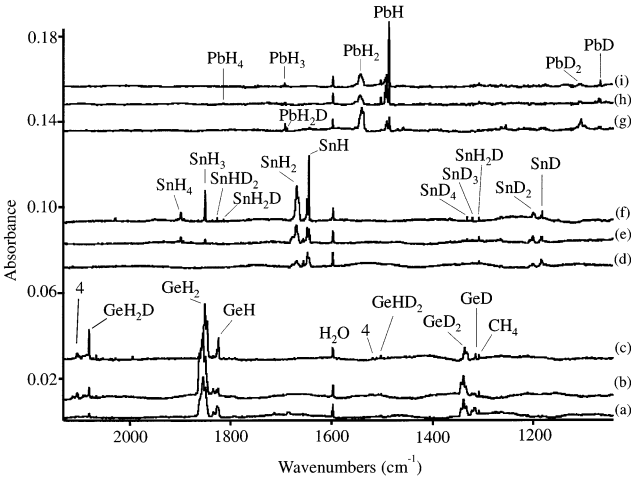

Figure 2. Infrared spectra in the 2130−1040 cm^{-1} region for laser-ablated Ge, Sn, or Pb co-deposited at 3.5 K with 2.5 mmol of a 50/50 H_2/D_2 mixture: (a) Ge + H_2/D_2, (b) after $\lambda > 240$ irradiation, (c) after annealing to 8.0 K, (d) Sn + H_2/D_2, (e) after $\lambda > 240$ nm irradiation, (f) after annealing to 7.7 K, (g) Pb + H_2/D_2, (h) after $\lambda > 240$ nm irradiation, (i) after annealing to 6.7 K.

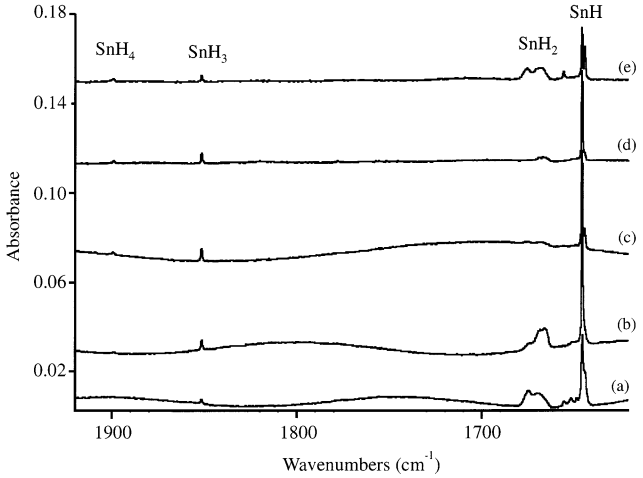

Figure 3. Infrared spectra in the 1920−1620 cm^{-1} region for laser-ablated Sn co-deposited at 3.5 K for 25 min with 2.5 mmol of normal hydrogen: (a) Sn + H_2, (b) after annealing to 6.3 K, (c) after $\lambda > 290$ nm irradiation, (d) after annealing to 6.5 K, and (e) after $\lambda > 240$ nm irradiation.

(37) Becerra, R.; Boganov, S. E.; Egorov, M. P.; Nefedov, O. M.; Walsh, R. *Chem. Phys. Lett.* **1996**, *260*, 433.
(38) Becerra, R.; Boganov, S. E.; Egorov, M. P.; Faustov, V. I.; Nefedov, O. M.; Walsh, R. *Can. J. Chem.* **2000**, *78*, 1428.
(39) Hassanzadeh, P.; Andrews, L. *J. Phys. Chem.* **1992**, *96*, 6181.
(40) B3LYP/6-311++G** calculation: Ge−H, 1.543 Å; Ge−Ge, 2.527 Å; Ge−H′, 1.597 Å; Ge−Ge−H, 113.8°; Ge−Ge−H′, 89.0°, 2112 cm^{-1} (163 km/mol), 2095 (139), 2084 (111), 1885 (272), 894 (29), 878 (40), 789 (264), 642 (41), . . .
(41) Ricca, A.; Bauschlicher, C. W., Jr. *J. Phys. Chem. A* **1999**, *103*, 11121.
(42) Levin, I. W.; Ziffer, H. *J. Chem. Phys.* **1965**, *43*, 4023.
(43) Halonen, M.; Halonen, L.; Bürger, H.; Sommer, S. *J. Phys. Chem.* **1990**, *94*, 5222.

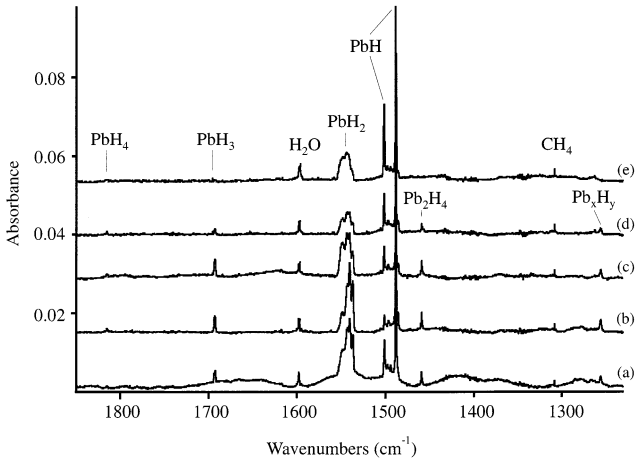

Figure 4. Infrared spectra in the 1850−1230 cm^{-1} region for laser-ablated Pb co-deposited at 3.5 K for 25 min with 2.5 mmol of normal hydrogen: (a) Pb + H_2, (b) after annealing to 6.1 K, (c) after $\lambda > 530$ nm irradiation, (d) after $\lambda > 290$ nm irradiation, and (e) after $\lambda > 240$ nm irradiation.

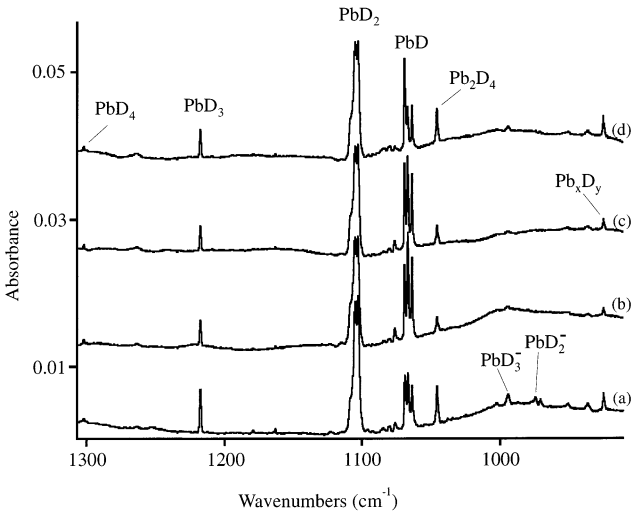

Figure 5. Infrared spectra in the 1305−910 cm^{-1} region for laser-ablated Pb co-deposited at 3.5 K for 25 min with 2.5 mmol of deuterium: (a) Pb + D_2, (b) after 240−380 nm photolysis, (c) after annealing to 7.2 K, and (d) after annealing to 9.0 K.

1.3922 and 1.3923 frequency ratios with the 1364.4 and 486.6 cm^{-1} deuterium matrix SnD_4 counterparts.[4]

The weak 911.7 cm^{-1} absorption increases on annealing and correlates with 912.9 and 905 cm^{-1} neon and argon matrix counterparts for Sn_2H_2 assigned previously on the basis of Sn_2H_2, Sn_2HD, and Sn_2D_2 substitution and DFT frequency calculations to the dibridged Sn_2H_2 ring species.[4,44] The 911.7/665.3 = 1.3704 H/D ratio is virtually the same as the neon matrix counterparts for this strong b_2 mode of Sn_2H_2. The weaker b_1 mode at 1117.8 cm^{-1} in neon is observed here at 1114.2 cm^{-1}. Because of the large yield of SnH in the pure hydrogen experiments, Sn_2H_2 is probably made here by dimerization of SnH.

Tin was reacted with a 50/50 H_2/D_2 mixture, and the spectrum (Figure 2d) again shows major products with 2/1 relative intensities that are appropriate for equal populations of SnH_2, SnH and SnD_2, SnD. This ratio is maintained on photolysis, but annealing markedly favored the hydrides over the deuterides. We note that SnH (1645.1 cm^{-1}) and SnD (1181.4 cm^{-1}) are slightly shifted from pure H_2 and pure D_2 values. Annealing also favored SnH_4, SnH_3 over SnD_4, SnD_3 and made possible the observation of sharp weak bands for SnH_3D (1893.5, 1864.3 cm^{-1}), SnH_2D (under SnH_3, 1814.4, 1320.7 cm^{-1}), $SnHD_3$ (1352.0 cm^{-1}), and $SnHD_2$ (under SnD_3, 1827.1, 1310.3 cm^{-1}), which are supported by DFT isotopic frequency calculations.

Lead. Five matrix isolation experiments were performed to search for laser energy and hydrogen deposition conditions (rate, duration) for maximum lead hydride product absorbance. Infrared spectra are illustrated in Figures 4 and 5 in the upper and lower regions. We observe a strong sharp 1488.3 cm^{-1} absorption for PbH, which fits into the trend 1504.6 cm^{-1} (gas phase), 1502.3 cm^{-1} (neon matrix), 1472.3 cm^{-1} (argon matrix) and exhibits the 1488.3/1063.9 = 1.3989 ratio with the PbD absorption in solid deuterium.[4,45] Note that there is a small matrix shift between solid hydrogen and deuterium: the sharp H_2O absorption appears at 1598.1 and 1597.3 cm^{-1} in solid H_2 and D_2, respectively.

Strong absorptions at 1543.7, 1540.7, 1537.1 cm^{-1} are due to PbH_2: the major 1540.6 cm^{-1} peak exhibits the 1540.6/1105.1 = 1.3941 ratio with the major PdD_2 absorption in solid deuterium. The hydrogen matrix 1540.7 cm^{-1} band is intermediate between the 1548.2 cm^{-1} neon matrix and 1532.7 cm^{-1} argon matrix PbH_2 values, and the calculated antisymmetric Pb−H_2 stretching frequency using the B3LYP density functional, 1605.0 cm^{-1}, requires a 0.961 scale factor to match the observed value.[4] A weak, broad 703 cm^{-1} band appears to be due to the bending mode of PbH_2 calculated at 753.8 cm^{-1} (B3LYP, Table 2). Earlier argon matrix experiments in this laboratory[4] revealed a weak 702 cm^{-1} band that tracked with PbH_2 on annealing and photolysis and a weak 501 cm^{-1} counterpart for PbD_2. The blue shoulder which often appears on the MH_2 absorption in these experiments is probably due to the $(H_2)MH_2$ complex intermediate in the reaction to form MH_4 product as characterized by quantum chemical calculations.[46]

A weaker absorption split at 1693.4, 1692.4 cm^{-1} is due to the ν_3(e) mode of the plumbyl radical first observed in solid neon and argon at 1697.7 and 1683.8 cm^{-1}, respectively.[4] This absorption exhibits a 1692.9/1217.4 = 1.3906 ratio with PbD_3 in solid deuterium and requires a 0.954 scale factor to fit the B3LYP frequency. Annealing the solid hydrogen sample first to 6.1 K slightly increased the 1693 cm^{-1} band (Figure 4b). Although ($\lambda > 530$ nm) mercury arc radiation had no effect, ultraviolet ($\lambda > 290$ nm) radiation decreased the 1693 cm^{-1} band by 70%, and $\lambda > 240$ nm radiation destroyed it, but weak 1815 cm^{-1} absorption remained (Figure 4c−e). A weaker 632.3 cm^{-1} absorption ($A = 0.0004$ as compared to 0.0016 for the 1693 cm^{-1} band) increased on annealing and decreased on photolysis with the 1693 cm^{-1} band, and the 632.3 cm^{-1} band is assigned to the ν_4(e) fundamental of PbH_3. The B3LYP functional predicts this mode with 0.942 scale factor and 20% of the intensity of ν_3(e) (Table 2). The weaker $\nu_2(a_1)$ mode predicted 4 cm^{-1} lower is not observed. A sharp 457.2 cm^{-1} band in the D_2 experiment, 632.3/457.2 = 1.3830 ratio, tracks

(44) Figure 6 in ref 4 incorrectly gives the H−M−H angle for Ge_2H_2: the correct angle is 70.0° as listed in the table for Sn_2H_2.

(45) Huber, K. P.; Herzberg, G. *Molecular Spectra and Molecular Structure. IV. Constants of Diatomic Molecules*; Van Nostrand Reinhold: New York, 1979.

(46) Pak, C.; Rienstra-Kiracofe, J. C.; Schaefer, H. F., III. *J. Phys. Chem. A* **2000**, *104*, 11232 and references therein.

Table 2. Frequencies and Bond Lengths Calculated at the DFT/6-311++G**/SDD Level for Lead Hydrides

	B3LYP[a]	BPW91[a]
PbH $^2\Pi$	1601.8, 1.843 Å (589)	1567.5, 1.856 Å (505)
PbH_2 $^1A_1$ C_{2v}	1605.0, 1603.3, 753.8 (b_2, 536), (a_1, 624), (a_1, 53) 1.839 Å, 90.8°	1571.6, 1568.7, 727.0 (537), (a_1, 469), (a_1, 41) 1.851 Å, 90.3°
PbH_3 $^2A_1$ C_{3v}	1775.0, 1703.6 (e 364 × 2), (a_1, 56) 671.6, 667.2 (e, 71 × 2), (a_1, 99) 1.769 Å, 109.1°	1732.1, 1647.4 (317 × 2), (52) 646.6, 638.5 (60 × 2), (78) 1.781 Å, 109.2°
PbH_4 $^1A_1$ T_d	1880.8, 1873.7 (0), (268 × 3) 740.9, 670.2 (e, 0 × 2), (t_2, 171 × 3) 1.743 Å	1828.0, 1815.3 (242 × 3), (0) 716.2, 640.0 (0), (137 × 3) 1.753 Å
Pb_2H_6 $^1A_{1g}$ D_{3d}	1846.4, 1832.1, 1827.2 (e_u, 657 × 2), (e_g, 0), (a_{1g}, 0) 1818.5, 709.1, 704.8, (a_{2u}, 416), (e_u, 117 × 2), (e_g, 0) 701.4, 587.8, 416.4, ...[b] (a_{1g}, 0), (a_{2u}, 800), (e_g, 0)	1800.8, 1788.5, 1774.9, (2 × 459), (0 × 2), (0) 1768.1, 689.0, 668.1, (396), (92 × 2), (0 × 2) 683.9, 573.7, 414.1, ...[b] (0), (800), (0 × 2)
$H(Pb_2H_2)H$ ^1A_g C_{2h}	1597.9, 1581.8, 1169.7, (a_u, 1030), (a_g, 0), (a_g, 0) 1093.0, 917.7, 904.5, (a_u, 1817), (a_g, 0), (a_u, 253) 699.8, 660.9, 533.6, ...[b] (a_u, 134), (a_g, 0), (a_g, 0) 1.840, 2.050 Å	1559.7, 1544.0, 1145.5 (885), (0), (0) 1091.7, 973.8, 912.1, (1467), (0), (197) 655.4, 623.2, 536.9, ...[b] (88), (0), (0) 1.853, 2.054 Å
PbH_3PbH $^1A_1$ C_s	1778 (376), 1775 (318), 1765 (376), 1615 (421), 718 (48), 716 (52), 664 (485), 505 (38), ...	
Pb_2H_2 $^1A_1$ C_{2v}	1159.5, 1079.5, 865.7 (a_1, 49), (b_1, 201), (b_2, 349) 718.8, 618.8, 131.7 (a_2, 0), (a_1, 81), (a_1, 1) 2.057, 2.906 Å H−Pb−H: 71.3° Pb−H−Pb: 89.9°	1144.6, 1078.3, 885.1 (42), (159), (325) 768.0, 600.3, 130.8 (0), (64), (1) 2.066, 2.912 Å, H−Pb−H: 71.2° Pb−H−Pb: 89.6°

[a] Infrared intensities (km/mol) given in parentheses under frequencies (cm^{-1}). [b] Three lower real frequencies omitted.

with the 1217.4 cm^{-1} PbD_3 absorption, and the former is due to ν_4 of the PbD_3 radical.

A very weak new absorption observed at 1815.0 cm^{-1} on sample deposition increased 50% on sample annealing to 6.1 K. Photolysis with red light had no effect, but $\lambda > 530$ nm radiation increased the 1815.0 cm^{-1} band to $A = 0.0008$ (Figure 4c). Subsequent $\lambda > 470$, $\lambda > 380$, and $\lambda > 290$ nm irradiations had no effect, but $\lambda > 240$ nm photolysis reduced the 1815.0 cm^{-1} band by one-half and destroyed the PbH_3 band. In addition, irradiation at $\lambda > 290$ nm markedly reduced PbH_2, but $\lambda > 240$ nm photolysis regenerated PbH_2.

The lower region (Figure 5) revealed a sharp 1459.2 cm^{-1} band, a broader 1255.7 cm^{-1} absorption, and sharp 978.2, 966.9, 959.5, and 789.4 cm^{-1} bands, which exhibited different annealing and photolysis behaviors.

Four experiments with pure deuterium revealed the strong 1063.9 cm^{-1} PbD absorption, the site-split PbD_2 band at 1105.1 cm^{-1}, and the sharp PbD_3 absorption at 1217.4 cm^{-1}. In addition, a new weak 1302.0 cm^{-1} absorption ($A = 0.0004$) increased 50% on 240−380 nm photolysis, increased to $A = 0.0007$ on annealing to 7.2 K, and decreased to $A = 0.005$ on annealing to 9.0 K (Figure 6). In a separate experiment, the final $\lambda > 240$ nm irradiation decreased the 1302.0 cm^{-1} band and destroyed the 1217.4 cm^{-1} absorption, and a final 8.0 K annealing slightly increased the 1302.0 cm^{-1} band and reproduced the 1217.4 cm^{-1} absorption. Absorptions in the lower region given in Table 1 are deuterium counterparts of the above bands.

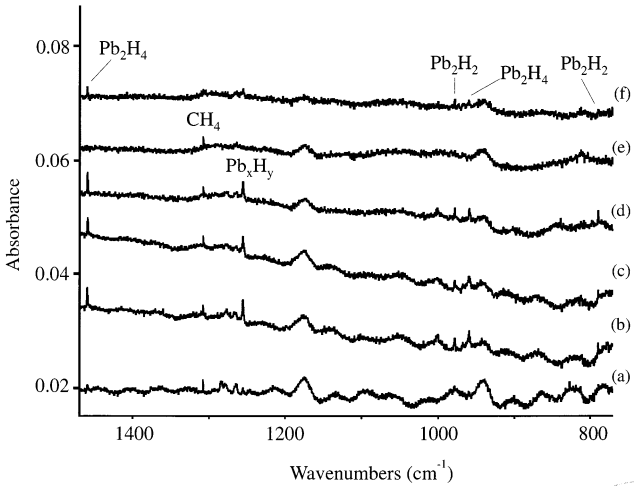

Figure 6. Infrared spectra in the 1470−770 cm^{-1} region for laser-ablated Pb co-deposited at 3.5 K for 25 min with 2.5 mmol of normal hydrogen: (a) Pb + H_2, (b) after annealing to 6.5 K, (c) annealing to 6.6 K, (d) after $\lambda > 290$ nm irradiation, (e) after $\lambda > 240$ nm irradiation, and (f) after annealing to 6.8 K.

Three 50/50 mixed H_2/D_2 experiments were conducted with lead, and the sample deposition spectrum in Figure 2g reveals PbH_2/PbD_2 absorbance in the ratio 3/1 and PbH/PbD absorbance with the ratio 5/1 (the computed infrared intensity ratio is 2/1). Photolysis ($\lambda > 240$ nm) increased monohydrides at the expense of dihydrides, but increased these ratios to 4/1 and 7/1, respectively, and 6.7 K annealing increased the ratios still further to 5/1 and 10/1. These observations show a clear preference for the Pb reaction with H_2 rather than D_2 first on deposition, more on UV photolysis, and even more on annealing to allow diffusion and reaction of H and D atoms. In this experiment, a weak 1814.8 cm^{-1} band, a strong 1692.0 cm^{-1} absorption with new 1687.5 and 1644.3 cm^{-1} satellites, and a sharp 631.5 cm^{-1} band were observed. The satellite peaks are due to the PbH_2D radical, and the 1692.0 and 631.5 cm^{-1} bands are due to PbH_3 in this 50/50 H_2/D_2 environment. In addition, a weak 1382.6 cm^{-1} absorption was observed for PbH_3^-. A 25/75 mixed H_2/D_2 sample gave analogous results, but the relative lead hydride band absorbance was 3-fold weaker with 25/75 H_2/D_2 relative to the 50/50 mixture.

Finally, a similar experiment was done with lead and H_2 containing 0.5% O_2. The fundamentals of HO_2 were observed at 3416.4 ($A = 0.0016$), 1392.7 ($A = 0.0055$), and 1100.7 cm^{-1} ($A = 0.0030$) in solid hydrogen, which are near the neon and argon matrix values.[47−49] In addition, a strong (ν_3) ozone band[50] was observed at 1037.8, 1034.6 cm^{-1} with a weak ($\nu_1 + \nu_3$) band at 2103 cm^{-1}. No lead oxide bands were detected.[26]

The 1815.0 cm^{-1} band is assigned to the ν_3 (t_2) mode of PbH_4 for the following reasons. First, the 1815 cm^{-1} band is in the region predicted by quantum chemical calculations[4,8] for ν_3 of

(47) Milligan, D. E.; Jacox, M. E. *J. Chem. Phys.* **1963**, *38*, 2627.
(48) Smith, D. W.; Andrews, L. *J. Chem. Phys.* **1974**, *60*, 81.
(49) Thompson, W. E.; Jacox, M. E. *J. Chem. Phys.* **1989**, *91*, 3826.
(50) Andrews, L.; Spiker, R. C., Jr. *J. Phys. Chem.* **1972**, *76*, 3208.

PbH_4. The 0.969 scale factor produces the observed band from our B3LYP calculated frequency for PbH_4, which is near the 0.961 scale factor found for PbH_2 in solid hydrogen. Second, the 1815 cm^{-1} band exhibits the same mechanistic behavior in these experiments as the 1899.5 and 2104.9 cm^{-1} absorptions for SnH_4 and GeH_4, an increase in selective photolysis and growth on annealing in parallel to the MH_3 radicals. Third, a similar weak 1302.0 cm^{-1} absorption in solid deuterium experiments defines a 1815.0/1302.0 = 1.3940 ratio and is the deuterium counterpart absorption of PbD_4 prepared here for the first time. Finally, the 1815 cm^{-1} hydrogen matrix band is in very good agreement with the gas-phase 1823 cm^{-1} band origin[3] recently assigned to PbH_4. Furthermore, the rotational constant B_3 measured for PbH_4 as 2.0694 cm^{-1} is in excellent agreement with our B3LYP calculated value of 2.0656 cm^{-1}. In the rigid-rotor approximation for a spherical top PbH_4 molecule, this B_3 value gives a Pb−H bond length of 1.741 Å, and our B3LYP calculation finds 1.743 Å. The authors estimate a 1.73 ± 0.01 Å equilibrium bond length from rotational analysis.[3] Such excellent agreement between hydrogen matrix, gas-phase,[3] and calculated[4,8] spectra for PbH_4 confirms the existence of this reactive tetrahydride molecule.

The sharp 789.4 cm^{-1} absorption increases on annealing to 6.1 K, decreases on visible photolysis, disappears on UV irradiation which produces PbH, and restores in part on further annealing. A new 575.9 cm^{-1} band with D_2 is counterpart (789.4/575.9 = 1.371). This band follows the trend of assignments to the antisymmetric b_2 stretching mode for doubly bridged Si_2H_2, Ge_2H_2, and Sn_2H_2, and it falls 8.8% below the B3LYP calculated b_2 mode for Pb_2H_2 or Pb(μ-H)$_2$Pb. The b_2 mode for Sn_2H_2 at 911.7 cm^{-1} is 6.0% below the B3LYP value (H/D ratio 1.369). Accordingly, the 789.4 cm^{-1} band is assigned to Pb_2H_2. The associated 978.2 cm^{-1} band (60% as intense) shows the same annealing and photolysis behavior and is 9.4% below the B3LYP value for the b_1 mode of Pb_2H_2. Accordingly, the 978.2 and 789.4 cm^{-1} bands are assigned to the two antisymmetric Pb−H−Pb stretching modes of Pb_2H_2. The doubly bridged structure illustrated in Figure 7 is similar to that calculated earlier for Pb_2H_2, Sn_2H_2, Ge_2H_2, and Si_2H_2.[4,23,33,34]

The large yield of PbH_2 in these experiments invites consideration of its dimer as a product species. Evidence for Ge_2H_4 was discussed above (Figure 1). Early SCF calculations[24] favored a doubly bridged structure over the trans-bent form for Pb_2H_4, and our DFT calculations reach the same conclusion. We also calculated the plumbyl plumbylene (PbH_3PbH) isomer and found it to be 11.2 kcal/mol above the doubly bridged structure, and the frequencies do not match our observed bands. Figure 7 shows a ring core for the most stable HPb(μ-H)$_2$PbH isomer similar to that found for Pb_2H_2 itself using the B3LYP density functional. Our structure is similar to that calculated at the SCF level.[24] The trans-ring C_{2h} structure is 1.4 kcal/mol more stable than the C_{2v} ring structure, but they have nearly the same calculated frequencies; similar results were found at the SCF level.[24] The strongest IR band is the calculated antisymmetric a_u ring mode at 1093 cm^{-1} with the second strongest b_u terminal mode at 1598 cm^{-1}, which is below the calculated frequency for PbH and clearly different from the relative frequencies for the Ge_2H_4 product.

The spectra in Figure 5 show that the 1459.2 and 959.5 cm^{-1} bands increase slightly on 6.1 K annealing, decrease on photolysis (with PbH_2), and restore on final annealing. With H_2/D_2 mixtures, 1458.6, 1046.2, and 962.3 cm^{-1} bands exhibit new 1469.0, 1052.3, and 971.7 cm^{-1} satellite absorptions that have the same annealing and photolysis behavior. These small shifts on the former bands are due to the different (50/50 H_2/D_2) matrix environment, but the new satellite features are due to mixed isotopic molecules for a higher hydride product. The new 1469.0 and 1052.3 cm^{-1} bands above the strong b_u modes of H(Pb_2H_2)H and D(Pb_2D_2)D are likely due to H(Pb_2HD)D, and they indicate that the forbidden a_g mode is higher than the b_u mode by a small amount opposite to the prediction of calculations. Previous neon and argon matrix spectra revealed 1463.3 and 1455.3 cm^{-1} bands identified as a late annealing product, but these spectra also contain associated 967 and 958.7 cm^{-1} absorptions. In the argon matrix spectrum, these two bands appear on 19 K annealing, increase then decrease on 25 and 30 K annealing, decrease on $\lambda > 240$ nm irradiation, and restore on 25 K annealing. On the basis of annealing and photolysis behavior and general agreement with the calculated frequencies, the above bands are assigned to the doubly bridged H(Pb_2H_2)H species. The trans-ring C_{2h} structure H(Pb_2H_2)H is 15.8 kcal/mol more stable than the trans-bent C_{2h} $H_2Pb-PbH_2$ structure, and the strongest frequencies of the latter, predicted in the 1600 cm^{-1} region, were not observed. Furthermore, the latter structure is a 24 kcal/mol higher energy saddle point at the SCF level.[24]

This work completes the group 14 M_2H_4 series except for Sn_2H_4 and shows that Pb_2H_4 has a nonplanar doubly bridged structure, in contrast to the trans-bent structures[34,36] observed for Ge_2H_4 and Si_2H_4 and the planar structure for C_2H_4.

The 1255.7 cm^{-1} band exhibits a 924.7 cm^{-1} D_2 counterpart and low H/D = 1.358 ratio and behavior similar to that of the 1459.2 cm^{-1} absorption. The argon matrix counterpart at 1247.1 cm^{-1} is much weaker, as diffusion is more difficult in the more

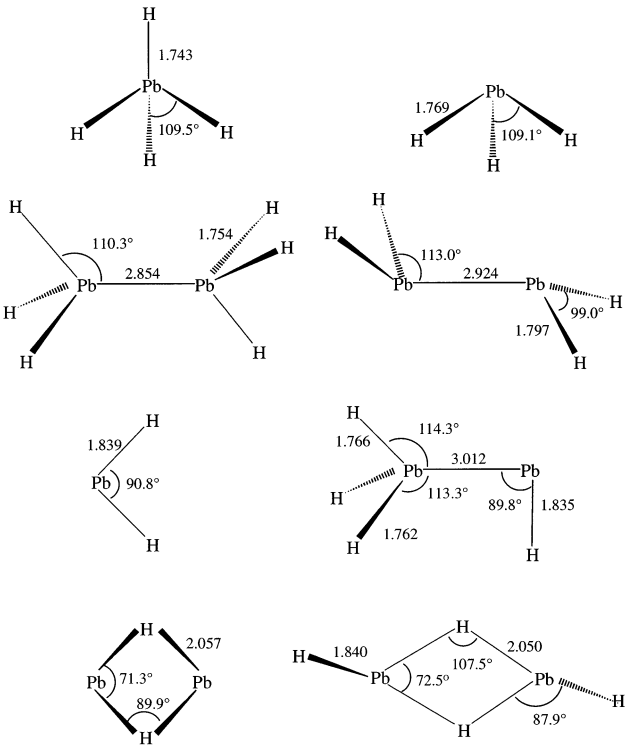

Figure 7. Structures calculated for lead hydrides at the B3LYP/6-311++G**/SDD level.

rigid argon matrix, and this band is likely due to a larger aggregate species involving a more anharmonic vibration. Finally, we converged a stable D_{3d} structure for Pb_2H_6 with the strongest Pb−H (e_u) stretching mode 27 cm^{-1} below the strong t_2 mode of PbH_4. We find no absorptions in this region presumably due to the low yield of PbH_3 radicals. A doubly bridged Pb_2H_6 structure of C_{2h} symmetry has an imaginary b_u frequency and is 101 kcal/mol higher in energy.

Reaction Mechanisms. The hydrogen matrix experiment is effectively a neon matrix experiment with very high H_2 concentration, which allows a high H atom concentration from photodissociation by vacuum ultraviolet radiation in the emission plume generated on the target surface by the laser pulse. Reactions 1−6 occur during co-deposition of H_2 and laser-ablated Pb atoms, which have sufficient excess energy[51] to activate reactions 1 and 2. Successive exothermic H atom addition reactions 3−6 occur in the matrix on annealing to allow diffusion and reaction of H atoms. On the basis of the gas-phase dissociation energy of PbH,[42] the B3LYP energies given for reactions 3−6 are probably too high. The formation of H atoms is attested by the observation of HO_2 in a H_2, 0.5% O_2 experiment. The relatively high concentration of H atoms in the H_2 matrix accounts for the observation of PbH_4 here in solid hydrogen but not in previous neon matrix experiments.[4]

$$Pb + H_2 \rightarrow PbH + H \qquad (\Delta E \geq 67 \text{ kcal/mol}) \qquad (1)$$

$$Pb + H_2 \rightarrow PbH_2 \qquad (\Delta E = -20 \text{ kcal/mol}) \qquad (2)$$

$$Pb + H \rightarrow PbH \qquad (\Delta E = -58 \text{ kcal/mol}) \qquad (3)$$

$$PbH + H \rightarrow PbH_2 \qquad (\Delta E = -60 \text{ kcal/mol}) \qquad (4)$$

$$PbH_2 + H \rightarrow PbH_3 \qquad (\Delta E = -35 \text{ kcal/mol}) \qquad (5)$$

$$PbH_3 + H \rightarrow PbH_4 \qquad (\Delta E = -68 \text{ kcal/mol}) \qquad (6)$$

Photochemical reaction 7 contributes to the formation of MH_2 in these experiments, and further reaction with the matrix cage provides more MH_4. In the case of 50/50 H_2/D_2, the photochemical reaction with H_2 in the matrix cage is favored by kinetic isotope effects.

$$M + H_2 \xrightarrow{h\nu} MH_2 \qquad (7)$$

$$MH_2 + H_2 \xrightarrow{h\nu} MH_4 \qquad (8)$$

The doubly bridged diplumbyne and diplumbene species are formed here through dimerization reactions 9 and 10. Further H atom reactions with Pb_2H_2 may also contribute to the yield of Pb_2H_4. Our B3LYP energy change for reaction 10 may be compared with −31 and −29 kcal/mol values at the SCF and CI levels, respectively.[24]

$$2PbH \rightarrow Pb_2H_2 \qquad (\Delta E = -44 \text{ kcal/mol}) \qquad (9)$$

$$2PbH_2 \rightarrow H(Pb_2H_2)H \qquad (\Delta E = -27 \text{ kcal/mol}) \qquad (10)$$

The rate of the primary reaction 2 or 7 obviously depends on the metal atomic state, and we have no control over that in the laser-ablation process. However, with constant laser energy, the yield of silicon hydride products is the highest of the four elements investigated here. When given the choice of H_2 or D_2 in a 50/50 H_2/D_2 experiment, only the least reactive lead shows a clear preference for hydrogen over deuterium.

Bonding Considerations. Much of the theoretical interest in PbH_4 stems from relativistic effects in the bonding.[5−13] Now that the same experimental measurement has been made on both PbH_2 and PbH_4, the ν_3 antisymmetric stretching modes at 1537 and 1815 cm^{-1}, respectively, in solid hydrogen, a new comparison of lead hydride molecules can be made. Although Pb(IV) compounds are strongly destabilized relative to Pb(II) compounds by electronegative substituents,[10] and relativistic lowering of the Pb 6s orbital contributes to the destabilization,[5] PbH_4 and PbH_2 appear to behave differently. In addition to bond length contraction and a frequency increase from PbH_2 to PbH_4, the average bond energy also increases (10−14% depending on the calculation).[9,10] Schwerdfeger et al.[9] report calculations of atomization energies where relativistic effects cause a 27−30% decrease for PbH_2 but only a 23−25% decrease for PbH_4. It is interesting to find that the ν_3 fundamental of PbH_4 is substantially higher (278 cm^{-1}) than the ν_3 mode of PbH_2, whereas the analogous difference for SnH_4 and SnH_2 is 235 cm^{-1}. From the energetic point of view, for lead hydrides, the IV state is preferred over the II state.[6]

Conclusions

Laser-ablated Si, Ge, Sn, and Pb atoms react with pure hydrogen on co-deposition at 3.5 K to form hydrides. The initial SiH_2 product reacts completely to SiH_4, whereas substantial proportions of GeH_2, SnH_2, and PbH_2 are trapped in solid hydrogen. Further hydrogen atom reactions lead to the trihydride radicals and tetrahydrides of Ge, Sn, and Pb. The observation of PbH_4 at 1815 cm^{-1} and PbD_4 at 1302 cm^{-1} is in agreement with the prediction of quantum chemical calculations for these unstable tetrahydride analogues of methane. In addition, new absorptions for Pb_2H_2 and $H(Pb_2H_2)H$ are observed, which have novel dibridged structures, based on quantum chemical calculations, in contrast to the well-known π-bonded structures of acetylene and ethylene.

Acknowledgment. We gratefully acknowledge support for this work from NSF Grant CHE 00-78836 and helpful correspondence with K. Faegri and P. Pyykkö.

JA029862L

(51) Kang, H.; Beauchamp, J. L. *J. Phys. Chem.* **1985**, *89*, 3364.